ISSN: 2093-5374 / E-ISSN: 2093-5382

Smart Medical Application of Deep Learning (MUNet) for Detection of COVID-19 from Chest Images

Ahmad AL Smadi[1*], Dr. Ahed Abugabah[2], Mutasem K. Al-smadi[3], and Ahmad Mohammad Al-smadi[4]

[1*]Department of Data Science and Artificial Intelligence, Zarqa University, Zarqa, Jordan.
aalsmadi@zu.edu.jo, https://orcid.org/0000-0003-3487-8041

[2]College of Technological Innovation, Zayed University, Abu Dhabi, UAE.
ahed.abugabah@zu.ac.ae, https://orcid.org/0000-0002-3181-5822

[3]Department of Management of Information Systems, College of Applied Studies and Community Service, Imam Abdulrahman Bin Faisal University, Dammam, Saudi Arabia.
mkalsmadi@iau.edu.sa, https://orcid.org/0000-0001-6892-8399

[4]Applied Science Department, Ajloun University College, Al-Balqa Applied University, Jordan.
amhs1966@bau.edu.jo, https://orcid.org/0000-0003-0126-0800

Received: September 11, 2023; Revised: November 15, 2023; Accepted: January 14, 2024; Published: March 30, 2024

Abstract

Fighting the outbreak of COVID-19 is now one of humanity's most critical matters. Rapid detection and isolation of infected people are crucial for decelerating the disease's spread. Due to the pandemic, the conventional technique for COVID-19 detection, reverse transcription-polymerase chain reaction, is time-consuming and in small abundance. Therefore, studies have been searching for alternate methods for detecting COVID-19, and thus applying deep learning methods to patients' chest images has been rendering impressive performance. The primary objective of this study is to suggest a technique for COVID-19 detection in chest images that is both efficient and reliable. We propose a deep learning method for COVID-19 classification based on a modified UNet called (Covid-MUNet). The Covid-MUNet model is trained using publicly available datasets, including chest X-ray images for multi-class classification (3-class and 4-classes) and CT scans images for binary/multi-class classification (2-classes and 3-classes). Using chest images, the Covid-MUNet is a successful methodology that helps physicians rapidly identify patients with COVID-19, thereby delaying the fast spread of COVID-19. The proposed model achieved an overall accuracy of 97.44% in classifying three categories (COVID-19, Normal, and Pneumonia) and an accuracy of 96.57% in classifying two categories (COVID-19 and Normal).

Keywords: Deep Learning, COVID-19, Medical Image Diagnosis, Image Classification, UNet, X-Ray Images, CT-scans.

1 Introduction

Over 200 countries worldwide have been significantly impacted by the coronavirus disease (COVID-19) outbreak. The COVID-19 pandemic emerged as a global crisis, sweeping across borders

Journal of Wireless Mobile Networks, Ubiquitous Computing, and Dependable Applications (JoWUA), volume: 15, number: 1 (March), pp. 133-153. DOI: *10.58346/JOWUA.2024.I1.010*

*Corresponding author: Department of Data Science and Artificial Intelligence, Zarqa University, Zarqa, Jordan.

and affecting millions of people and disrupting economies, healthcare systems, and daily life (Abugabah, A., 2023). As coronavirus is very contagious, it spreads swiftly among people sick with COVID-19 (Corona Virus Disease– 19). The virus spreads via nasal discharge and saliva droplets when a person infected with COVID-19 tingles or sneezes. A person infected with COVID-19 could have a dry cough, muscular soreness, headache, fever, sore throat, and mild to moderate respiratory illness. However, older persons and those with preexisting medical conditions such as coronary artery disease, asthma, and cancer are more likely to develop serious infections. As the pneumonia form's source of infection is unknown and a new virus might be formed via mutation, it is challenging for COVID-19 patients to identify a vaccine or therapy. According to the WHO, more research and socioeconomic inequities within the community in highly notified areas of different nations afflicted by the corona pandemic are recommended. In order to evaluate COVID-19 results, estimate their severity, or identify other illness etiologies, physicians may conduct X-rays/CT-scan modalities for patients. Which may contribute to medical therapy or supporting therapeutic choices, such as hospitalization, a demand for monitoring, or anticipation of disease risks, and will modify the focus of COVID-19 treaters via radiographic examinations (Rahman, S., 2021). Using such modalities can readily identify the radiological properties of COVID-19. X-ray scans of the chest cannot precisely distinguish soft tissues (Al Smadi, A., 2022). Thereby, a chest CT scan is used to identify soft tissues effectively. Chest CT scans must be evaluated by radiologists (Yasar, H., 2021). Numerous radiologists are needed to diagnose COVID-19 in this pandemic circumstance. Nonetheless, it is costly in time and an error-prone procedure. Consequently, the automated identification of COVID-19 on chest images is necessary (Mehmood, A., 2022). Deep learning methods have been extensively used in the detailed automated examination of medical imagery (Singh, D., 2020) (Al Smadi, A., 2022) (Sharma, P., 2023) (Sharma, A., 2022) (Huyut, M.T., 2023). A study conducted by (Huyut, M.T., 2023) based on feed forward neural network demonstrated that COVID-19 infection could be identified by integrating routine blood values with the LogNNet method (Velichko, A. 2021). This approach substantiates the notion that routine blood values carry significant information crucial for detecting COVID-19 (Nizam et al., 2023).

It turned out that applied deep learning might be used for disease detection in chest images (Tingting, Y., 2019). Deep learning is more versatile and efficient than RT–PCR because it automatically learns features from data (Fourcade, A., 2019). In view of that, the deep learning methods can be conducted on a large dataset of chest images by training the weights of networks or on small datasets using fine-tuning the weights of pre-trained networks (Owida, H.A., 2022). Researchers have found the effectiveness of deep learning for COVID-19 classification from chest images (Owida, H.A., 2022).

Therefore, pre-trained neural networks may be used for coronavirus diagnosis from CT-Scans or X-Ray images. And numerous approaches based on deep learning have been presented, with promising results in terms of detecting COVID-19-infected individuals using chest images. These approaches have exclusively concentrated on chest X-Rays or CT scans (Wang, L., 2020) (Das, D., 2020) (Montalbo, F. J.P., 2021) (Montalbo, F.J.P., 2021) (Gunraj, H., 2020) (Polsinelli, M., 2020) (Wang, S., 2021) (Xu, X., 2020) (Li, L., 2020) (Abugabah, A., 2022); only a small percentage of these approaches used both types of chest images (Ibrahim, D.M., 2021) (Montalbo, F.J., 2022) (Khan, A.I., 2020). In this study, we propose a deep learning method for COVID-19 classification based on a modified UNet called (Covid-MUNet). Using chest images, the Covid-MUNet is a successful methodology that helps physicians rapidly identify patients with COVID-19, thereby delaying the fast spread of COVID-19. The Covid-MUNet model is trained using publicly available datasets, including chest X-ray images for multi-class classification (3-class and 4-classes) and CT scans images for binary/multiclass classification (2-classes and 3-classes). In addition, we estimated the COVID-M-UNet model's performance in terms

of six metrics, including precision, sensitivity, specificity, F1-score, accuracy, and Matthew's correlation coefficient (MCC) (Shichkina et al., 2020).

2 Related Work

Numerous studies have been conducted to identify the COVID-19 by radiological imaging. According to the research of Wang et al. (Wang, L., 2020), they started their attempt to identify chest X-rays by gathering data from a variety of trustworthy sources. Their research devised a customized convolutional neural network that detects X-ray images using many linked layers that extracted characteristics and then inputted into a set of fully linked neural networks. This method used a parameter size of around 11.75 million and achieved an overall accuracy of 93.3%. Narin et al. (Narin, A., 2021) used three DL models (ResNet50, InceptionV3, and Inception-ResNetV2) for binary-class classification to detect Covid-19 in infected patients and conducted on three different datasets. They attained an accuracy of 98% by using ResNet50. In (Chowdhury, M. E., 2020), four pre-trained networks models, ResNet18, AlexNet, SqueezeNet, and DenseNet201, were utilized. Moreover, an augmentation process was used for training data. Thus, attained an accuracy of 98% in 3-class classification. Hemdan et al. (Hemdan, E.E.D., 2020) presented a COVIDX-Net model, which encompasses seven unique deep architectures for the purpose of COVID-19 identification. This method was conducted on a dataset with 2-classes and attained an accuracy of 90% (Ozyilmaz 2023).

Another significant study, "ULNet", was presented in (Wu, T., 2021). It used X-ray imaging to detect COVID-19 in infected patients. This model was run on a single dataset, which included both two-class and three-class classifications. For the two-class classification, it had an accuracy of 99.53%, and for the three-class classification, it had an accuracy of 95.35%. Apostolopoulos et al. (Apostolopoulos, I.D., 2020) introduced a technique for detecting Covid-19 based on deep learning. This method obtained an aggregate two-class accuracy of 98.75% and a three-class accuracy of 93.48%.

In a recent study, Sharma et al. (Sharma, P., 2023) proposed the implementation of Conv-CapsNet, a novel approach utilizing capsule networks, in order to identify individuals infected with COVID-19. The Conv-CapsNet model boasted an impressive parameter count of 23 million and was evaluated using a 5-fold cross-validation technique. The results demonstrated an overall accuracy of 96.47% for multi-class classification and 97.69% for binary classification. In a related study, the author (Sharma, A., 2022) fused the MobileNetV2 and VGG16 models to create a novel "COVDC-Net" to detect COVID-19 infection in individuals. The COVDC-Net model demonstrated an overall classification accuracy of 96.48% for the 3-class classification task and 90.22% for the 4-class classification task.

Qzturk et al. (Ozturk, T., 2020) proposed the DarkCovid-Net model for covid-19 diagnosis based on chest X-ray images and attained an accuracy of 98.08% for the 2-class classification and 87.02% for the 3-class classification. Tawsifur et al. (Rahman, T., 2021) proposed a DenseNet201 model and attained an accuracy for three classes of 95.11%. Panwar et al. (Panwar, H., 2020) introduced the nCOVnet model and the results revealed that the nCOVnet model has an overall accuracy of 88%. Das et al. (Das, D., 2020) proposed a DL-based model which lowered the required cost (2.1M parameters) for the work without a decrease in performance of the multi-classification of X-ray images. The experiments revealed 99.92% of classification accuracy. Montalbo (Montalbo, F.J.P., 2021) employed another approach to Covid-19 detection based on DenseNets, and the analysis yielded favorable outcomes, demonstrating a high level of accuracy at 97.99% and a minimal parameter need of 1.2 M. The aforementioned cited investigations were limited to Chest X-Rays and did not address the diagnosis of COVID-19 infected lung CT images.

In (Gunraj, H., 2020), the authors developed the COVIDNet-CT model, which was built mainly for diagnosing CT scans. The COVIDNet-CT model produced a 99.1% accuracy rate with 1.4 million parameters for multi classification. Sarker et al. (Sarker, L., 2020) classified COVID-19 patients based on CT scan images using DenseNet-121. They employed transfer learning to eliminate the gradient issue while training the deep learning network. They created a website that extracts diseased zones from radiological scans. This approach had an 87% accuracy rate. Shan et al. (Shan, F., 2020) introduced a DL-based classification method for automatically identifying infected lung tissues. They examined their method on 300 individuals infected with the coronavirus. This approach yielded a 91% accuracy rate. Zhang et al. (Zhang, J., 2020) used the DenseNet model to classify Covid-19. The classification sensitivity of the employed model for COVID-19 and non-COVID-19 cases is 96% and 70.65%, respectively. Wang et al. (Wang, S., 2020) employed a pre-trained DL method for detecting COVID-19. This method was implemented on 1,266 patients and had an 87% accuracy rate. Gozes et al. (Gozes, O., 2020) proposed a DL approach to identify and measure the extent of COVID-19 severity in chest CT images. Techniques such as segmentation, slice classification, and grain localization were used. Lung-infected areas are segmented using UNet and classified using ResNet, respectively. This approach yielded an accuracy of 94.0% after testing over 110 affected people. In (Wang, S., 2021), the authors classified COVID-19 in lung CT scan images using InceptionNet. The model was assessed using a dataset consisting of 1065 CT images, from which 325 people were classified as COVID-19, with an accuracy rate of 85.2%. Chen et al. (Chen, J., 2020) detected Covid-19 with UNet++ architecture, and it was trained on 106 cases and exhibited an accuracy of 98.85%. In (Zheng, C., 2020), a DeCovNet approach for leveraging 3D CT images to diagnose COVID-19 patients. In which a pre-trained UNet approach was utilized for the segmentation. Their model yielded an accuracy of 95.9%. Li et al. (Li, L., 2020) presented ResNet50-based COVNet model. The findings revealed that the model's specificity and sensitivity for classifying COVID-19 were 96% and 90%, and the overall accuracy was 0.96%. Song et al. (Song, Y., 2021) built a DL model named Deep Pneumonia for COVID-19 classification. The highest accuracy attained in this model was 94% for binary classification (Amiruzzaman et al., 2022).

The CoroNet model was introduced by Khan et al. (Khan, A.I., 2020), and the model was conducted on both chest X-ray/CT images. This model had an overall accuracy of 95% for 3-classes and 89.6% for 4-classes. Authors in Ref. (Ibrahim, D.M., 2021), developed a Deep-chest model for diagnosing COVID-19 using both chest X-ray/CT images. This model's experiments revealed that it was trained for 500 and 800 epochs to attain the highest possible ratings. Thus, it attained an accuracy rate of 98.05% using a parameter size of about 22.3 million. Moreover, (Montalbo, F.J., 2022) developed a truncation approach based on tuning and pre-training to detect Covid-19 using both chest X-ray/CT images in infected patients. This model attained an accuracy of 97.41% and reduced the size of a parameters to 44K.

It's worth noting that Ref (Ibrahim, D.M., 2021) was conducted on one curated dataset for infected lungs that includes 4-classes (COVID-19, Pneumonia, Lung Cancer, and Normal), whereas Ref (Montalbo, F.J., 2022) was conducted on a curated dataset with 6-classes (Normal Chest X-ray, COVID-19 X-ray, Pneumonia X-ray, Normal Chest CT scan, COVID-19 CT scan, and Pneumonia CT scan). Our goal is to leverage the strengths of the U-Net architecture, such as its ability to capture both local and global features, and apply them to the classification of Covid-19 images. To this end, and to make use of the advantages given by deep learning techniques, we enhance the classification accuracy in this study. A comprehensive Covid-MUNet is proposed for identifying Covid-19 in infected patients. It is evaluated on chest imaging comprising CT/X-rays, unlike most previous studies concentrating on one chest image type or just a binary classification.

3 Method Details

In this section, we present Covid-MUNet, an innovative deep-learning network that utilizes the well-recognized U-net architecture for detecting COVID-19 in chest X-ray/CT scans images. Fig. 1 depicts the architecture of the Covid-MUNet network. U-net (Ronneberger, O., 2015) was introduced in 2015, it has been extensively used in medical image. This is primarily attributed to its exceptional network design. However, Covid-MUNet is an upgraded structure of U-net that is used for classification tasks to detect COVID-19 in infected patients. The proposed network architecture is depicted in Table 1.

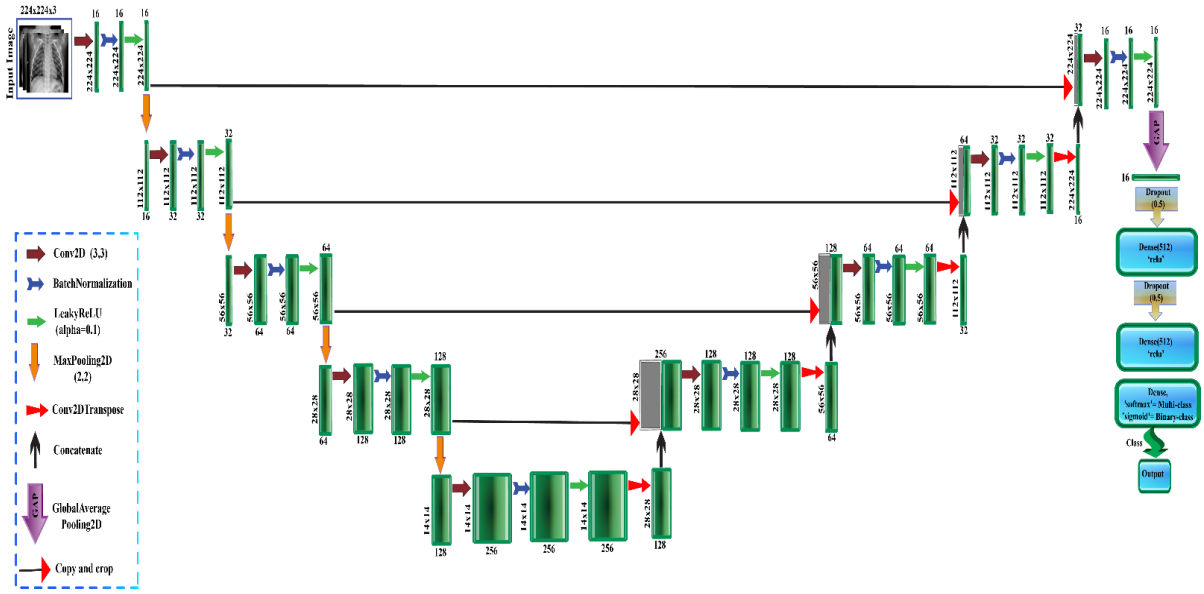

Figure 1: Flowchart of proposed Covid-MUNet model

The Covid-MUNet structure network is essentially identical to the U-net structure, with the addition of a batch normalization layer following each convolutional layer and using Leaky ReLU activation (instead of a level slope, the negative values have a slight slope), and a batch normalization layer which is crucial for its advantages such as helps speed the network's convergence rate, regulate the gradient explosion, and reduce overfitting (Ioffe, S., 2015). Each convolutional block is fundamentally composed of three operations: convolution, batch normalization, and activation layer. The Covid-MUNet network's down sampling structure boosts the network's depth to acquire deep-level features. Skip links between the up-sampling and the down-sampling are used. By merging different layers of features, these skip connections save a significant amount of data loss caused by the pooling procedure. Global Average Pooling is used, a benefit of global average pooling over completely linked layers is that it is more natural to the convolution structure since it enforces correspondences between feature maps and categories. Additionally, there is no parameter to optimize in global average pooling, therefore overfitting is prevented at this layer. Moreover, global average pooling totals the spatial information, making it more resistant to spatial translations of the input (Lin, M., 2013). The last fully connected layer is transmitted to a 'Sigmoid' function in the binary-classification and a 'Softmax' function in the multi-classification. In short, our Covid-MUNet model includes a convolutional layer with activation units and batch normalization, as well as deconvolution and dense layers. We describe these components in detail below.

Table 1: The proposed Covid-MUNet architectures

Layer	Type	Output Shape	# Parameters
	Input	(None, 224, 224, 3)	0
Conv1	Conv2D	(None, 224, 224, 16)	448
BN1	BatchNormalization	(None, 224, 224, 16)	64
ReLU1	LeakyReLU	(None, 224, 224, 16)	0
Pool1	MaxPooling2D	(None, 112, 112, 16)	0
Conv2	Conv2D	(None, 112, 112, 32)	4640
BN2	BatchNormalization	(None, 112, 112, 32)	128
ReLU2	LeakyReLU	(None, 112, 112, 32)	0
Pool2	MaxPooling2D	(None, 56, 56, 32)	0
Conv3	Conv2D	(None, 56, 56, 64)	18496
BN3	BatchNormalization	(None, 56, 56, 64)	256
ReLU3	LeakyReLU	(None, 56, 56, 64)	0
Pool3	MaxPooling2D	(None, 28, 28, 64)	0
Conv4	Conv2D	(None, 28, 28, 128)	73856
BN4	BatchNormalization	(None, 28, 28, 128)	512
ReLU4	LeakyReLU	(None, 28, 28, 128)	0
Pool4	MaxPooling2D	(None, 14, 14, 128)	0
Conv5	Conv2D	(None, 14, 14, 256)	295168
BN5	BatchNormalization	(None, 14, 14, 256)	1024
ReLU5	LeakyReLU	(None, 14, 14, 256)	0
Up6	Conv2DTranspose	(None, 28, 28, 128)	295040
Concat6	Concatenate	(None, 28, 28, 256)	0
Conv6	Conv2D	(None, 28, 28, 128)	295040
BN6	BatchNormalization	(None, 28, 28, 128)	512
ReLU6	LeakyReLU	(None, 28, 28, 128)	0
Up7	Conv2DTranspose	(None, 56, 56, 64)	73792
Concat7	Concatenate	(None, 56, 56, 128)	0
Conv7	Conv2D	(None, 56, 56, 64)	73792
BN7	BatchNormalization	(None, 56, 56, 64)	256
ReLU7	LeakyReLU	(None, 56, 56, 64)	0
Up8	Conv2DTranspose	(None, 112, 112, 32)	18464
Concat8	Concatenate	(None, 112, 112, 64)	0
Conv8	Conv2D	(None, 112, 112, 32)	18464
BN8	BatchNormalization	(None, 112, 112, 32)	128
ReLU8	LeakyReLU	(None, 112, 112, 32)	0
Up9	Conv2DTranspose	(None, 224, 224, 16)	4624
Concat9	Concatenate	(None, 224, 224, 32)	0
Conv9	Conv2D	(None, 224, 224, 16)	4624
BN9	BatchNormalization	(None, 224, 224, 16)	64
ReLU9	LeakyReLU	(None, 224, 224, 16)	0
GAP	GlobalAveragePooling2D	(None, 16)	0
Dense1	Dense	(None, 512)	8704
Dropout1	Dropout	(None, 512)	0
Dense2	Dense	(None, 512)	262656
Dropout2	Dropout	(None, 512)	0
Output	Dense	(None, 3)	1539
Total Parameters			1,452,291

3.1. Convolution and Transposed Convolutional Layers

The convolutional layer is the most fundamental component of a CNN. It contains a set of filters whose parameters must be learnt during the training procedure. Typically, filters are less in size than the original image. Each filter generates an activation map by convergently processing the image. The filter is applied across the vertical and horizontal dimensions of the image, and the dot product between each element of the filter and the corresponding element of the input is calculated at each spatial point (LeCun, Y., 2010). Whereas the deconvolution or fractionally stridden convolutions layers "Transposed Convolutions" perform a conventional convolution but revert its spatial conversion (Dumoulin, V., 2016), enlarging the input image by adding zeros in a particular proportion.

3.2. Activation Function

The generally used activation functions are nonlinear. The categories of nonlinear activation functions vary. There are several variations of activation functions, the most common of which are the ReLU, Sigmoid, Softmax, Tanh, and Leaky ReLU. Sigmoid activation forecasts the likelihood within the interval 0 to 1. It is applicable to traditional ML methods. The Tanh activation operation is similar to the logistic sigmoid, with a range between -1 and 1 (Goodfellow, I.J., 2015). ReLU has shown to be better than its predecessor owing to the ease with which its partial derivative may be computed (Krizhevsky, A., 2017). The ReLU activation is the most prevalent of all CNN methods. ReLU does not let gradients vanish. Despite this, ReLU is less effective because of the huge gradient operator. This causes the neuron to deactivate, resulting in the death of ReLU. This issue may be resolved via Leaky ReLU (Maas, A.L., 2013). The sigmoid activation function generates Nonlinear output from the linear one, whereas the softmax activation function transforms the linear output into a probabilistic one (Nwankpa, C., 2018).

3.3. Batch Normalization Layer

Batch normalization is an operation that occurs after the convolution step. Its purpose is to normalize the inputs to the layers of a network by re-centering and rescaling the data. This makes the training of the network more efficient and stable. The process involves the first step of removing the mean of the minibatch, and then dividing the outcomes by the standard deviation of the minibatch. This normalizes each input channel throughout the whole minibatch.

3.4. Pooling Layer

CNN processing Pooling layers are often used to minimize the network's size, accelerate computation, and improve the robustness of certain detectable characteristics. As a result, there are several variations of pooling layers, the most common of which are Max Pooling, Average Pooling, Global Average Pooling, and Global Max Pooling. The pooling layer preserves the most important information while simultaneously down sampling and compressing features to limit the amount of work that must be done. In addition to this, the pooling layer has the capability of increasing the size of the receptive field. The pooling procedure involves moving a window of a certain size over the feature map in discrete stages. Our method used max-pooling between the convolutional blocks by taking the max within each filter, and the Global Average Pooling as a substitute for the Flatten layers. It generates one feature map for each classification task category corresponding to the final Conv layer.

3.5. Dense Layer (Fully Connected)

When a feature is retrieved from the front, it is linked to all the preceding nodes in a completely connected layer. Suppose an image dataset has more than one category. In that case, this feature vector will be longer than the length of the convolution layer's output feature map, which is typically the number of image categories. The input image's feature vector includes all of the image's information in one place. Although the image's location information is lost, the vector preserves the most distinctive aspects of the image to finish the image classification process. An image classification process requires just that a computer evaluate the content of an image and calculate a specified category probability value for that image, then provide a category that is the most probable match. Adam is one of the gradient descent optimization techniques. It is both widely used and very successful and is employed as the function for optimization in the proposed Covid-MUNet within the dense layer. A dropout layer is added after the dense layer to avoid overfitting. We use the relatively modest filter 3X3 because if a large filter is utilized, the receptive field will be too large. As a consequence, the majority of the information that is retrieved will be useless, which will lead to poor accuracy in classification.

4 Experimental Results and Analysis

Google Collaborative was used, which provides a free 1xTesla K80 GPU containing 12GB of GDDR5 VRAM and 2496 CUDA cores. Training time was significantly shortened thanks to GPU assistance in parallel processing. The model is trained across 50 epochs. Based on the confusion matrix (Sammut, C., 2017), multi-class classification measures are used to assess the model's capability. The proposed model has been conducted on three X-ray and two CT-Scans datasets. The model is used for binary classification (COVID-19 vs. Normal), three (COVID-19 vs. Normal vs. Pneumonia) classifications, as well as four classifications (COVID-19 vs. Normal vs. Viral Pneumonia vs. Lung Opacity). In order to enhance the models' adaptability and performance during training while minimizing computational requirements, a callback function known as Reduce LR on Plateau (RLRoP) was utilized in this study. Additionally, the application of early stopping allowed the model to cease training once the validation error reached its minimum point. Detailed hyperparameter configurations employed in the proposed methodology are presented in Table 2.

Table 2: Description of Hyperparameter Configuration

Hyperparameter	Values
Activation Function	LeakyReLU / Sigmoid / Softmax
Learning Rate	Base: 1e-3
	Minimum: 1e-5
Epochs	50
Batch Size	32
Optimizer	Adam
Loss Function	Binary Cross-Entropy (for binary classifier)
	Categorical Cross-Entropy (for multi-class classifier)
Early Stopping Patience	10
Monitoring Metric	Validation Accuracy
Learning Rate Schedule	Factor: 0.1
	RLRoP: 2

4.1. Experiments on X-rays Datasets

Three publicly available X-rays datasets were used for implementation: The dataset XR-Data-1 is categorized into three groups, namely COVID-19, Normal, and Pneumonia (Patel, P. 2020). The relative quantities of images for the COVID-19, Normal, and Pneumonia classes are 576, 1583, and 4273. The XR-Data-2 dataset (Asraf, A., 2020) is categorized into three groups, namely COVID-19, Normal, and Pneumonia, with a total of 6939 samples. Each category consists of 2313 samples. The dataset known as XR-Data-3 is referred to as the "Radiography Database." It has a total of 3616 instances of COVID-19-positive images, with 10192 images classified as Normal, 6012 images classified as Lung Opacity, and 1345 images classified as Viral Pneumonia (Rahman, T., 2020).

On XR-Data-1, three class classifications, the confusion matrix is shown in sub-Fig. 2(a), and Receiver operating curve (ROC) and Precision-Recall curve (PRC) are displayed in sub-Fig. 3(a). Additionally, the performance metrics were computed for each class (COVID-19, Normal, Pneumonia) and these metrics are reported in Table 3. On XR-Data-2, its corresponding confusion matrix is illustrated in sub-Fig. 2 (b), accompanied by the ROC and PRC curves are shown in sub-Fig. 3(b). Moreover, the performance metrics for each class are documented in Table 4. This insures a comprehensive analysis of the classification outcomes and model performance across both datasets.

On XR-Data-3, four class classifications, the confusion matrix is illustrated in sub-Fig. 2 (c). The ROC and PRC curves are demonstrated in sub-Fig. 3(c). Moreover, the performance metrics for each class are documented in Table 5. For a more comprehensive examination, the ROC curve shows the model's trade-offs between sensitivity and specificity. The PRC curve places a greater emphasis on inaccurate diagnoses than the ROC. The proposed method produced a good performance across all classes. The noticeable point appears that the lowest value in the ROC curve is 99%. In the PRC curve, the lowest value is 96% for class 1 on XR-Data-2. Moreover, we depicted the training and validation analyses of the proposed model throughout the training process' epochs, as shown in Fig. 4.

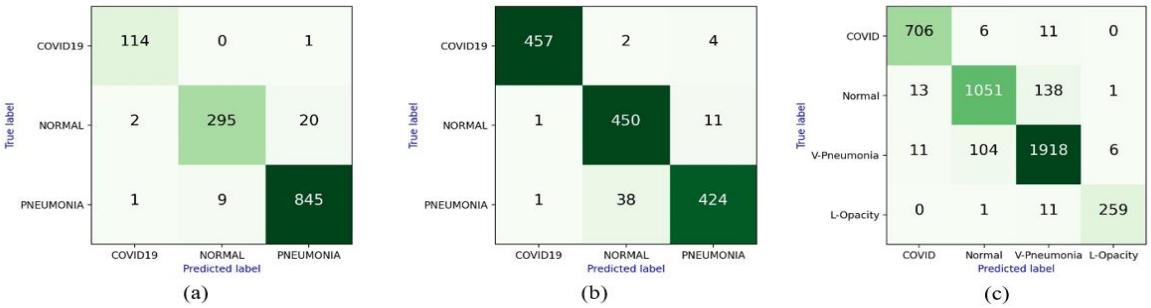

Figure 2: Confusion matrix of the proposed Covid-MUNet on X-ray Datasets. (a) XR-Data-1, (b) XR-Data-2, (c) XR-Data-3

Table 3: Evaluation performance of the proposed Covid-MUNet vs. UNet model on XR-Data-1

Covid-MUNet							
Class	**Accuracy**	**Sensitivity**	**Specificity**	**Precision**	**F1-score**	**MCC**	**Overall Acc (%)**
Covid-19	0.997	0.991	0.997	0.974	0.983	0.981	97.44
Normal	0.976	0.931	0.991	0.97	0.95	0.935	
Pneumonia	0.976	0.988	0.951	0.976	0.982	0.946	
UNet model							
Class	**Accuracy**	**Sensitivity**	**Specificity**	**Precision**	**F1-score**	**MCC**	**Overall Acc (%)**
Covid-19	0.971	0.939	0.974	0.783	0.854	0.842	91.6
Normal	0.949	0.890	0.969	0.904	0.897	0.863	
Pneumonia	0.939	0.938	0.942	0.970	0.954	0.867	

In Table 3, the Covid-MUNet model demonstrates superior performance compared to the UNet model on XR-Data-1. The Covid-MUNet achieves an overall accuracy of 97.44%, indicating its ability to classify images across all classes accurately. It outperforms the UNet model regarding MCC, F1-score, precision, specificity, sensitivity, and accuracy for all three classes. Moving on to Table 4, on XR-Data-2, the Covid-MUNet model continues to exhibit excellent performance. With an overall accuracy of 95.89%, it achieves high accuracy, sensitivity, specificity, precision, F1-score, and MCC for the Covid-19, Normal, and Pneumonia classes. In contrast, the UNet model lags behind in terms of accuracy and other performance metrics for all three classes.

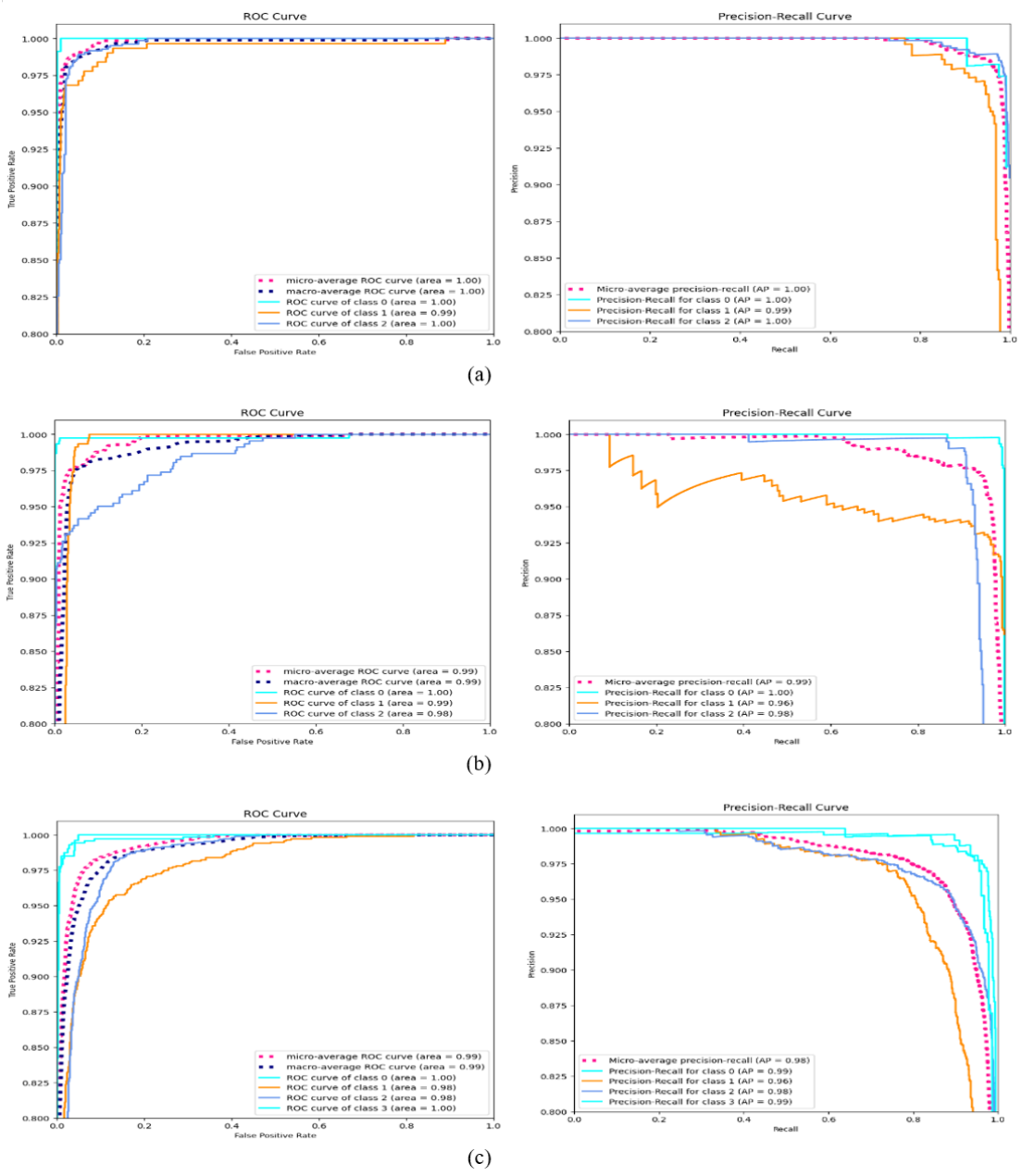

Figure 3: Receiver operating curve and Precision-Recall operating curve of the proposed Covid-MUNet on X-ray Datasets. (a) XR-Data-1, (b) XR-Data-2, (c) XR-Data-3

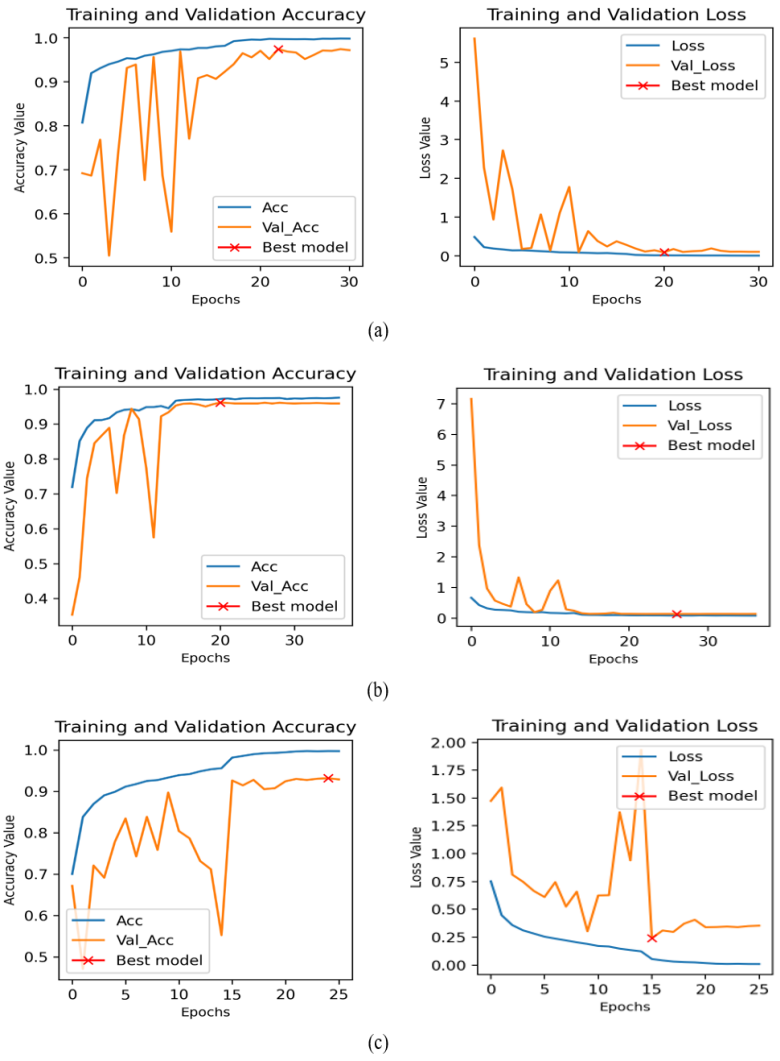

Figure 4: Proposed model training, validation accuracy, and loss for X-ray Datasets. (a) XR-Data-1, (b) XR-Data-2, (c) XR-Data-3

Table 4: Evaluation performance of the proposed Covid-MUNet vs. UNet model on XR-Data-2

Covid-MUNet							
Class	**Accuracy**	**Sensitivity**	**Specificity**	**Precision**	**F1-score**	**MCC**	**Overall Acc (%)**
Covid-19	0.994	0.987	0.998	0.996	0.991	0.987	95.89
Normal	0.963	0.974	0.957	0.918	0.945	0.918	
Pneumonia	0.961	0.916	0.984	0.966	0.94	0.912	
UNet model							
Class	**Accuracy**	**Sensitivity**	**Specificity**	**Precision**	**F1-score**	**MCC**	**Overall Acc (%)**
Covid-19	0.948	0.875	0.985	0.967	0.919	0.883	89.7
Normal	0.915	0.913	0.916	0.844	0.877	0.814	
Pneumonia	0.928	0.892	0.946	0.892	0.892	0.837	

Lastly, Table 5 displays the evaluation results on XR-Data-3. The Covid-MUNet model maintains its superior performance, achieving an overall accuracy of 95.87%. It demonstrates exceptional performance in terms of MCC, F1-score, precision, specificity, sensitivity, and accuracy for the Covid-19, Normal, Pneumonia, and Lung Opacity classes. Conversely, the UNet model falls short, showing lower accuracy and performance metrics for all classes. These findings highlight the effectiveness and robustness of the proposed Covid-MUNet model in accurately classifying chest X-ray images. The model consistently outperforms the UNet model across different datasets, demonstrating its potential for accurately diagnosing Covid-19, Normal cases, Pneumonia, and even Lung Opacity. The results validate the proposed model's superiority in classification accuracy, sensitivity, specificity, and overall performance.

Table 5: Evaluation performance of the proposed Covid-MUNet vs. UNet model on XR-Data-3

Covid-MUNet							
Class	**Accuracy**	**Sensitivity**	**Specificity**	**Precision**	**F1-score**	**MCC**	**Overall Acc(%)**
Covid-19	0.99	0.976	0.993	0.967	0.972	0.966	95.87
Normal	0.938	0.874	0.963	0.904	0.889	0.846	
Pneumonia	0.933	0.941	0.926	0.923	0.932	0.866	
Lung Opacity	0.996	0.956	0.998	0.974	0.965	0.962	
UNet model							
Class	**Accuracy**	**Sensitivity**	**Specificity**	**Precision**	**F1-score**	**MCC**	**Overall Acc(%)**
Covid-19	0.945	0.721	0.991	0.942	0.817	0.795	75.2
Normal	0.795	0.490	0.916	0.697	0.576	0.458	
Pneumonia	0.765	0.877	0.660	0.705	0.782	0.548	
Lung Opacity	0.982	0.911	0.986	0.821	0.864	0.855	

4.2. Experiments on CT-Scans datasets

In this section, two publicly available Ct-scan datasets were used for implementation. The first is the binary dataset (Soares, E., 2020) "SARS-CoV-2", which we named CT-Data-1. It contains 2481 CT scans, among them 1252 CT scans of patients with COVID-19 and 1229 CT scans non-infected by COVID-19. The second data is the multi-class CT scan dataset for COVID-19, which we named CT-Data-2. Two hospitals gathered this data in Brazil, which is publicly available in (Soares, E., 2020). In total, 4173 CT scans were collected, among them 2168 CT scans of patients with COVID-19, 758 CT scans non-infected by COVID-19, and 1247 CT scans performed for individuals with other pulmonary diseases.

The proposed Covid-MUNet and UNet models' evaluation performance on two different CT-Scan datasets, CT-Data-1 and CT-Data-2, is presented in Tables 6 and 7, respectively. In addition, Figs. 5, 6, and 7 provide visual representations of the model's performance and training progress.

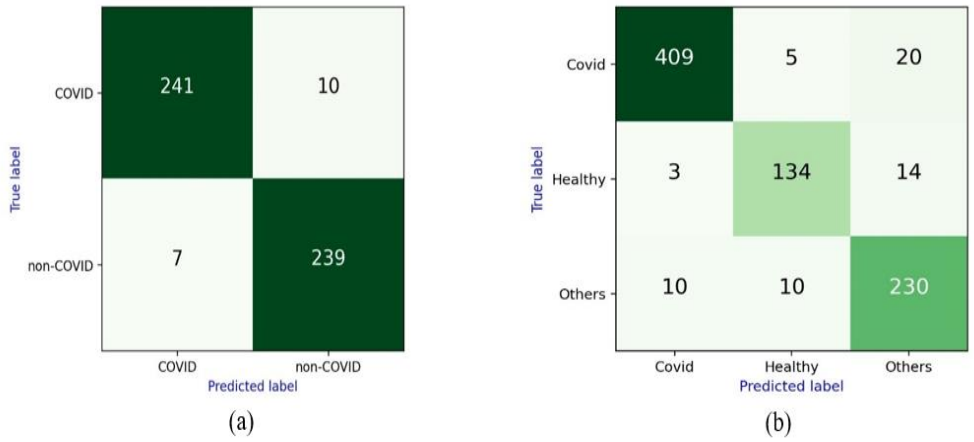

Figure 5: Confusion matrix of Covid-MUNet on CT-Scan Datasets. (a) CT-Data-1, (b) CT-Data-2

Table 6 illustrates the evaluation performance on CT-Data-1. The Covid-MUNet model achieves an overall accuracy of 96.57%. It outperforms the UNet model in terms of performance metrics for both Covid-19 and Normal classes. The UNet model, on the other hand, shows lower performance metrics.

Table 6: Evaluation performance of the proposed Covid-MUNet vs. UNet model on CT-Data-1

Covid-MUNet							
Class	**Accuracy**	**Sensitivity**	**Specificity**	**Precision**	**F1-score**	**MCC**	**Overall Acc (%)**
Covid-19	0.966	0.96	0.972	0.972	0.966	0.932	96.57
Normal	0.966	0.972	0.96	0.96	0.966	0.932	
UNet model							
Class	**Accuracy**	**Sensitivity**	**Specificity**	**Precision**	**F1-score**	**MCC**	**Overall Acc (%)**
Covid-19	0.628	0.514	0.744	0.672	0.582	0.265	
Normal	0.628	0.744	0.514	0.600	0.664	0.265	62.7

Moving on to Table 7, on CT-Data-2, the Covid-MUNet model maintains strong performance with an overall accuracy of 93.57%. It exhibits high MCC, F1-score, precision, specificity, sensitivity, and accuracy for Covid-19, Healthy, and others classes. In contrast, the UNet model again demonstrates inferior performance, with lower accuracy and performance metrics for all classes. Figs. 5 and 6 present the confusion matrix, (ROC), and (PR) curve for the Covid-MUNet model on CT-Data-1 and CT-Data-2. These figures provide visual insights into the model's classification performance and the trade-off between sensitivity and specificity. The Covid-MUNet model exhibits a higher area under the curve (AUC) in both the ROC and PR curves, indicating its superior performance compared to the UNet model.

Fig. 7 showcases the training and validation accuracy and loss curves for the proposed Covid-MUNet model on CT-Data-1 and CT-Data-2. The model consistently improves accuracy during training while the loss decreases over epochs. This indicates the model's ability to learn and make accurate predictions on the CT-Scan datasets. Overall, the results indicate that the proposed Covid-MUNet model outperforms the UNet model on both CT-Data-1 and CT-Data-2. The Covid-MUNet model demonstrates higher accuracy, MCC, F1-score, precision, specificity, and sensitivity for the target classes Covid-19, Normal, Healthy, and Others. The visual representations in the form of confusion matrices, ROC curves, PR curves, and training progress further support the superior performance and effectiveness of the proposed Covid-MUNet model in CT-Scan classification tasks.

Table 7: Evaluation performance of the proposed Covid-MUNet vs. UNet model on CT-Data-2

Covid-MUNet							
Class	**Accuracy**	**Sensitivity**	**Specificity**	**Precision**	**F1-score**	**MCC**	**Overall Acc (%)**
Covid-19	0.954	0.942	0.968	0.969	0.956	0.909	93.57
Healthy	0.962	0.887	0.978	0.899	0.893	0.87	
Others	0.935	0.92	0.942	0.871	0.893	0.849	
UNet model							
Class	**Accuracy**	**Sensitivity**	**Specificity**	**Precision**	**F1-score**	**MCC**	**Overall Acc (%)**
Covid-19	0.687	0.816	0.549	0.662	0.731	0.379	63.35
Healthy	0.855	0.570	0.918	0.606	0.587	0.500	
Others	0.725	0.356	0.882	0.563	0.587	0.278	

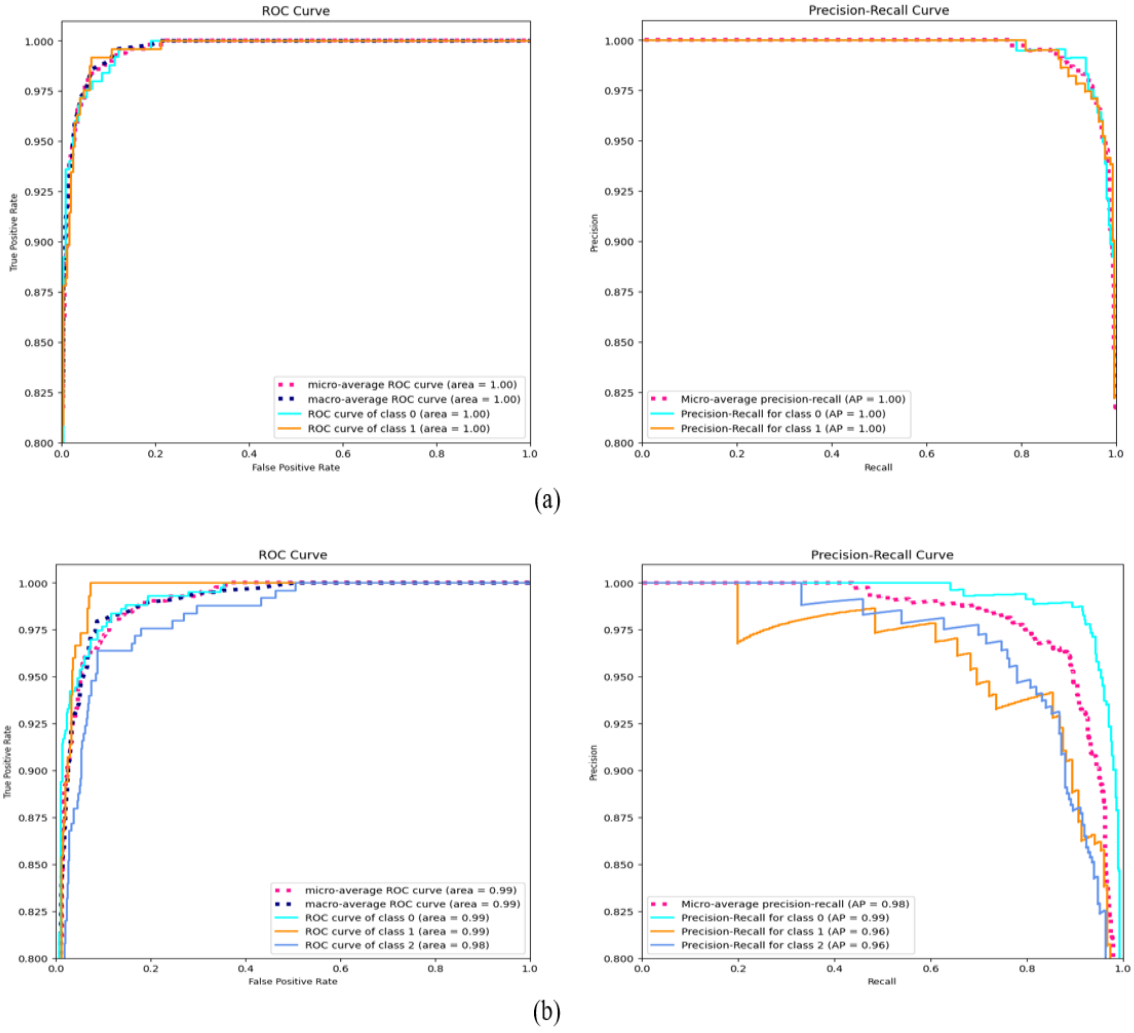

Figure 6: Receiver operating curve and Precision-Recall operating curve of the proposed Covid-MUNet on CT-Scan Datasets. (a) CT-Data-1, (b) CT-Data-2

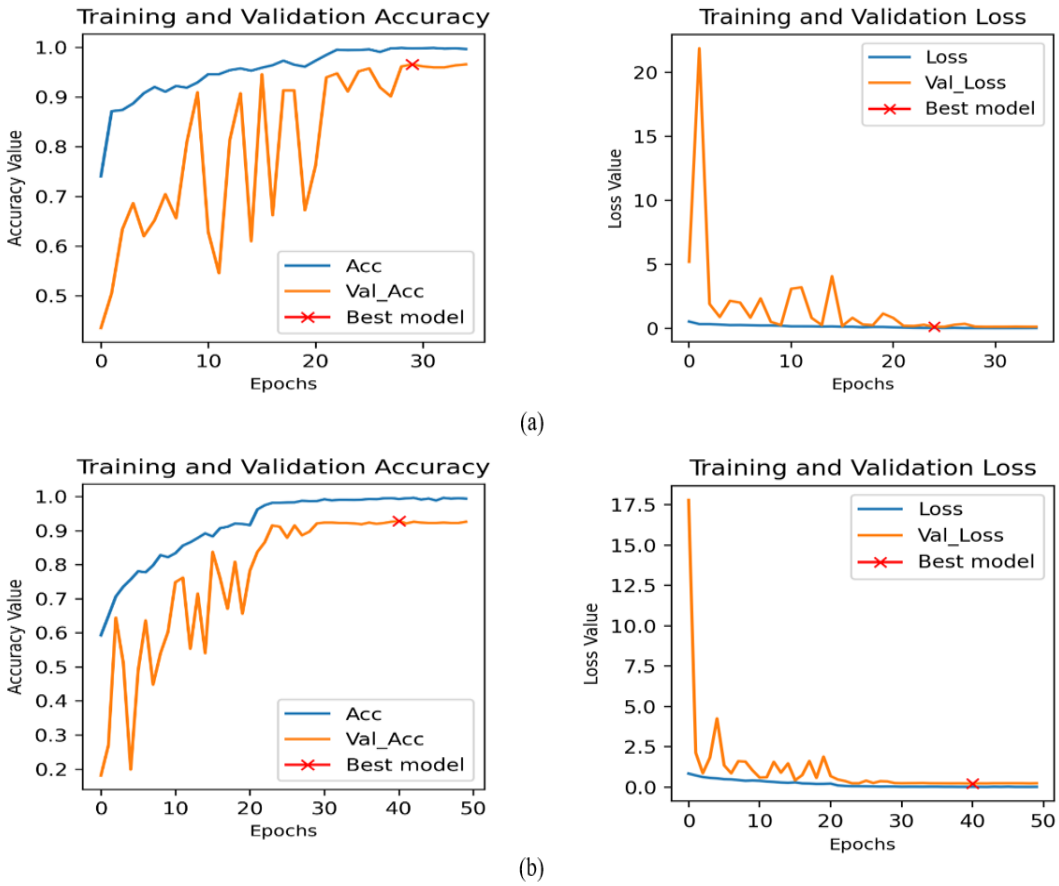

Figure 7: Proposed model training, validation accuracy, and loss for CT-Scan Datasets (a) CT-Data-1, (b) CT-Data-2

With the high cost of PCR testing, it was deemed beneficial to provide healthcare practitioners with an artificial intelligence-driven methodology for swiftly and precisely forecasting COVID-19. This paper presented a DL method based on UNet for the early diagnosis of COVID-19 using chest images. Our model's benefit is that it assigns a score to each class forecast and only transmits the highest-scoring prediction. Our model achieved superior performance concerning six quality measures and reduced the size of a parameter to ~1.45 million. With these findings, it can be established that the suggested model may be used to identify COVID-19 fast and accurately since it is able to differentiate between cases of pneumonia that are characteristic of COVID-19. Comparing the predictions of our model to those of the radiologist revealed a much greater degree of accuracy and sensitivity.

To provide context for our study, Table 8 presents an overview of relevant literature studies focused on diagnosing COVID-19 using chest X-ray and CT-scan images, highlighting a comparison with our proposed model. It is important to note that a direct comparison between our study and the referenced literature studies is challenging due to the different methodologies employed. Unlike the prior studies, which concentrated on a single modality (CT-scan or X-ray) and focused on binary or multi-class classification, our research was conducted using five distinct datasets comprising both X-ray and CT-scan images. Despite this distinction, the comprehensive analysis presented in Table 8 indicates that our Covid-MUNet technique yielded commendable results without the need for data augmentation or extensive training periods.

Furthermore, the scoring mechanism employed by our model sets it apart from other approaches. As depicted in Table 8, some studies (Wang, S., 2021) (Li, L., 2020) (Chen, J., 2020) utilized solely chest CT images for diagnosis. While studies such as (Ibrahim, D. M., 2021) (Montalbo, F. J., 2022) demonstrated promising outcomes, it is important to note that they required 500-800 epochs to achieve their results and were conducted on a single dataset comprising X-ray and CT images. In a nutshell, our proposed Covid-MUNet model showcased the potential of deep learning techniques in accurately detecting COVID-19 from chest images. The model's ability to assign scores to class predictions, superior performance across various evaluation metrics, and reduced parameter size make it a valuable tool for healthcare professionals. Future research may further explore the integration of additional datasets and modalities to enhance the proposed model's diagnostic capabilities.

Table 8: Comprehensive comparison between the proposed technique and many other current deep learning (DL) methods

Reference	**Imaging Type**	**Overall Performance (%)**	**Number of Epochs**	**Number of Parameters**
Montalbo, F. J., (2022)	X-ray and CT-scans (Normal, vs. COVID-19 vs. Pneumonia)	Accuracy of 97.41 Precision of 97.59 Sensitivity of 97.52 Specificity of 97.55	500 and 800	441 K
(Li, L., 2020)	CT Scans (COVID-19 vs. CAP vs. Non-Pneumonia)	Sensitivity of 90 Specificity of 96	N/A	25.6 M
(Xu, X., 2020)	CT Scans (COVID-19 vs. non-COVID-19)	Accuracy of 89.5 Sensitivity of 0.88 Specificity of 0.87	15,000	23 M
(Ibrahim, D. M., 2021)	CT Scans and X-Ray (Normal vs. Pneumonia vs. COVID-19 vs. Lung Cancer)	Accuracy of 98.05 Precision of 98.43 Sensitivity of 98.05 Specificity of 99.5 F1 score of 98.24 MCC of 97.7	800	22.3 M
(Wang, L., 2020)	X-ray (Normal vs. CAP vs. COVID-19)	Accuracy of 93.3	22	11.75 M
(Wu, T., 2021)	X-ray (COVID-19 vs. Normal vs. Viral Pneumonia)	2-class: Accuracy of 99.53% 3-class: Accuracy of 95.35%	60	N/A
(Chen, J., 2020)	CT Scans (COVID-19 vs. Normal)	Accuracy of 98.85 Sensitivity of 94.34 Specificity of 99.16	N/A	N/A
(Luz, E., 2021)	X-ray (Normal vs. COVID-19 vs. Pneumonia)	Accuracy of 93.51 Sensitivity of 96.8	20	23.2M
(Chhikara, P., 2021)	X-ray (Normal vs. COVID-19 vs. Pneumonia)	Accuracy of 97.70 Precision of 97.6 Sensitivity of 97.6 Specificity of 97.6	50	N/A
(Sharma, P., 2023)	X-ray (Normal vs. COVID-19 vs. Pneumonia)	2-class: Accuracy of 97.69%% 3-class: Accuracy of 96.47%	50	23M
(Sharma, A., 2022)	X-ray (COVID-19 vs. Healthy vs. Pneumonia) X-ray (COVID-19 vs. Healthy vs. Viral Pneumonia vs. Bacterial Pneumonia)	3-class: Accuracy of 96.48% 4-class: Accuracy of 90.22%	70 and 25	N/A
Covid-MUNet	X-ray (Normal vs. COVID-19 vs. Pneumonia) X-ray (COVID-19 vs. Normal vs. Viral Pneumonia vs. Lung Opacity) CT Scans (COVID-19 vs. Normal) CT Scans (COVID-19 vs. Healthy vs. Others)	Accuracy of 97.44 Sensitivity of 97.0 Specificity of 97.97 Precision of 97.33 F1-score of 97.17 MCC of 95.4	50	1.45 M

5 Conclusion

This study developed a binary/multi-classification deep learning model based on the UNet network and assessed for COVID-19 detection from chest x-ray and CT images. To establish the appropriate therapy and limit the spread of COVID-19, it is crucial to promptly and accurately diagnose these diseases and isolate COVID-19 patients. The proposed model showed superiority for Covid-19 detection in infected patients through extensive experiments and results on five publicly available datasets. Even though our model reduced the size of a parameter to ∼1.45 million, we observed that the performance of the proposed model could be used efficiently to diagnose COVID-19 cases from medical images. The proposed model achieved an overall performance 97.44% accuracy, 97.44% sensitivity, 97.0% specificity, 97.97% precision, 97.17% F1-score, 95.4% MCC, for 3-class classification on the X-ray dataset-1. In addition, for 3-class classification on the X-ray dataset-2, it attained an over- all performance 95.89% accuracy, 95.9% sensitivity, 97.97% specificity, 96.0% precision, 95.87% F1-score, 93.9% MCC. For 4-class classification on the X-ray dataset-3 had an overall performance of 95.87% accuracy, 93.68% sensitivity, 97.0% specificity, 94.2% precision, 93.95% F1-score, 91.0% MCC. Furthermore, our model achieved an overall performance 96.57% accuracy, 96.6% sensitivity, 96.6% specificity, 96.6% precision, 96.6% F1-score, 93.2% MCC, for binary-class classification on the CT-scan dataset-1. And for multi-class classification had an overall performance of 93.57%accuracy, 91.63% sensitivity, 96.23% specificity, 91.3% precision, 91.4% F1-score, and 87.6% MCC.

Funding Statement: This research is supported by Zayed University, Office of Research, RIF No R22050.

Author Contributions: AL. Ahmad; Conceptualization of this study, Methodology, Software, Writing - Original draft preparation. A. Ahed, A. Mutasem and A. Ahmad; Data curation, Investigation, Writing – review and editing. All authors reviewed the results and approved the final version of the manuscript.

Ethics Approval: Our work does not involve human subjects or animal experiments. The datasets used and analyzed during the current study are available from the corresponding author upon request.

Conflicts of Interest: The authors declare that they have no conflicts of interest to report regarding the present study.

References

[1] Abugabah, A., & Shahid, F. (2023). Intelligent Health Care and Diseases Management System: Multi-Day-Ahead Predictions of COVID-19. *Mathematics*, *11*(4), 1051. https://doi.org/10.3390/math11041051

[2] Abugabah, A., Mehmood, A., Al Zubi, A.A., & Sanzogni, L. (2022). Smart COVID-3D-SCNN: a novel method to classify X-ray images of COVID-19. *Computer Systems Science and Engineering*, *41*(3), 997-1008.

[3] Al Smadi, A., Abugabah, A., Al-Smadi, A.M., & Almotairi, S. (2022). SEL-COVIDNET: An intelligent application for the diagnosis of COVID-19 from chest X-rays and CT-scans. *Informatics in Medicine Unlocked*, *32*, 101059. https://doi.org/10.1016/j.imu.2022.101059

[4] Al Smadi, A., Abugabah, A., Mahenge, S.F., & Shahid, F. (2022). Information Systems in Medical Settings: A Covid-19 Detection System Using X-Ray Scans. *In 26th International Computer Science and Engineering Conference (ICSEC)*, 72-77.

[5] Amiruzzaman, M., Islam, M.R., Islam, M.R., & Nor, R.M. (2022). Analysis of COVID-19: An infectious disease spread. *Journal of Internet Services and Information Security (JISIS), 12*(3), 1-15.

[6] Apostolopoulos, I.D., & Mpesiana, T.A. (2020). Covid-19: automatic detection from x-ray images utilizing transfer learning with convolutional neural networks. *Physical and engineering sciences in medicine*, *43*, 635-640.

[7] Asraf, A. (2020). Balanced-X-Ray-dataset-3. *URL https://www.kaggle.com/amanullahasraf/covid19-pneumonia-normal-chest-xray-pa-dataset.*

[8] Chen, J., Wu, L., Zhang, J., Zhang, L., Gong, D., Zhao, Y., & Yu, H. (2020). Deep learning-based model for detecting 2019 novel coronavirus pneumonia on high-resolution computed tomography. *Scientific reports*, *10*(1), 19196. https://doi.org/10.1038/s41598-020-76282-0

[9] Chhikara, P., Gupta, P., Singh, P., & Bhatia, T. (2021). A deep transfer learning based model for automatic detection of COVID-19from chest X-rays. *Turkish Journal of Electrical Engineering and Computer Sciences*, *29*(8), 2663-2679.

[10] Chowdhury, M.E., Rahman, T., Khandakar, A., Mazhar, R., Kadir, M.A., Mahbub, Z.B., & Islam, M.T. (2020). Can AI help in screening viral and COVID-19 pneumonia?. *IEEE Access*, *8*, 132665-132676.

[11] Das, D., Santosh, K.C., & Pal, U. (2020). Truncated inception net: COVID-19 outbreak screening using chest X-rays. *Physical and engineering sciences in medicine*, *43*, 915-925.

[12] Dumoulin, V., & Visin, F. (2016). A guide to convolution arithmetic for deep learning. *arXiv preprint arXiv:1603.07285*.

[13] Fourcade, A., & Khonsari, R.H. (2019). Deep learning in medical image analysis: A third eye for doctors. *Journal of stomatology, oral and maxillofacial surgery*, *120*(4), 279-288.

[14] Goodfellow, I.J., Bengio, Y., & Courville, A.C. (2015). Deep learning. *Nature, 521,* 436–444.

[15] Gozes, O., Frid-Adar, M., Greenspan, H., Browning, P.D., Zhang, H., Ji, W., & Siegel, E. (2020). Rapid ai development cycle for the coronavirus (covid-19) pandemic: Initial results for automated detection & patient monitoring using deep learning ct image analysis. https://doi.org/10.48550/arXiv.2003.05037

[16] Gunraj, H., Wang, L., & Wong, A. (2020). Covid net-ct: A tailored deep convolutional neural network design for detection of covid-19 cases from chest ct images. *Frontiers in medicine*, *7*. https://doi.org/10.3389/fmed.2020.608525

[17] Hemdan, E.E.D., Shouman, M.A., & Karar, M.E. (2020). Covidx-net: A framework of deep learning classifiers to diagnose covid-19 in x-ray images. https://doi.org/10.48550/arXiv.2003.11055

[18] Huyut, M.T., & Velichko, A. (2023). LogNNet model as a fast, simple and economical AI instrument in the diagnosis and prognosis of COVID-19. *MethodsX*, *10*, 102194. https://doi.org/10.1016/j.mex.2023.102194

[19] Ibrahim, D.M., Elshennawy, N.M., & Sarhan, A.M. (2021). Deep-chest: Multi-classification deep learning model for diagnosing COVID-19, pneumonia, and lung cancer chest diseases. *Computers in biology and medicine*, *132*, 104348. https://doi.org/10.1016/j.compbiomed.2021.104348

[20] Ioffe, S., & Szegedy, C. (2015). Batch normalization: Accelerating deep network training by reducing internal covariate shift. *In International conference on machine learning*, 448-456.

[21] Khan, A.I., Shah, J.L., & Bhat, M.M. (2020). CoroNet: A deep neural network for detection and diagnosis of COVID-19 from chest x-ray images. *Computer methods and programs in biomedicine*, *196*, 105581. https://doi.org/10.1016/j.cmpb.2020.105581

[22] Krizhevsky, A., Sutskever, I., & Hinton, G.E. (2017). ImageNet classification with deep convolutional neural networks. *Communications of the ACM*, *60*(6), 84-90.

[23] LeCun, Y., Kavukcuoglu, K., & Farabet, C. (2010). Convolutional networks and applications in vision. *In Proceedings of IEEE international symposium on circuits and systems*, 253-256.

[24] Li, L., Qin, L., Xu, Z., Yin, Y., Wang, X., Kong, B., & Xia, J. (2020). Using artificial intelligence to detect COVID-19 and community-acquired pneumonia based on pulmonary CT: evaluation of the diagnostic accuracy. *Radiology*, *296*(2), E65-E71.

[25] Lin, M., Chen, Q., & Yan, S. (2013). Network in network. https://doi.org/10.48550/arXiv.1312.4400

[26] Luz, E., Silva, P., Silva, R., Silva, L., Guimarães, J., Miozzo, G., & Menotti, D. (2021). Towards an effective and efficient deep learning model for COVID-19 patterns detection in X-ray images. *Research on Biomedical Engineering*, 1-14.

[27] Maas, A.L., Hannun, A.Y., & Ng, A.Y. (2013). Rectifier nonlinearities improve neural network acoustic models. *In Proc. ICML*, *30*(1). http://robotics.stanford.edu/~amaas/papers/relu_hybrid_icml2013_final.pdf

[28] Mehmood, A., Abugabah, A., & Al Smadi, A. (2022). Smart health care system for early detection of COVID-19 using X-ray scans. *In international conference on electrical, computer and energy technologies (ICECET)*, 1-4.

[29] Montalbo, F.J. (2022). Truncating fined-tuned vision-based models to lightweight deployable diagnostic tools for SARS-CoV-2 infected chest X-rays and CT-scans. *Multimedia Tools and Applications*, *81*(12), 16411-16439.

[30] Montalbo, F.J.P. (2021). Diagnosing Covid-19 chest x-rays with a lightweight truncated DenseNet with partial layer freezing and feature fusion. *Biomedical Signal Processing and Control*, *68*, 102583. https://doi.org/10.1016/j.bspc.2021.102583

[31] Montalbo, F.J.P. (2021). Truncating a densely connected convolutional neural network with partial layer freezing and feature fusion for diagnosing COVID-19 from chest X-rays. *MethodsX*, *8*, 101408. https://doi.org/10.1016/j.mex.2021.101408

[32] Narin, A., Kaya, C., & Pamuk, Z. (2021). Automatic detection of coronavirus disease (covid-19) using x-ray images and deep convolutional neural networks. *Pattern Analysis and Applications*, *24*, 1207-1220.

[33] Nizam, M., Zaneta, S., & Basri, F. (2023). Machine Learning based Human eye disease interpretation. *International Journal of Communication and Computer Technologies (IJCCTS)*, *11*(2), 42-52.

[34] Nwankpa, C., Ijomah, W., Gachagan, A., & Marshall, S. (2018). Activation functions: Comparison of trends in practice and research for deep learning. https://doi.org/10.48550/arXiv.1811.03378

[35] Owida, H.A., Hemied, O.S.M., Alkhawaldeh, R.S., Alshdaifat, N.F.F., & Abuowaida, S.F.A. (2022). Improved Deep Learning Approaches for Covid-19 Recognition in CT Images. *Journal of Theoretical and Applied Information Technology*, *100*(13), 4925-4931.

[36] Owida, H.A., Migdadi, H.S., Hemied, O.S.M., Alshdaifat, N.F.F., Abuowaida, S.F.A., & Alkhawaldeh, R.S. (2022). Deep learning algorithms to improve COVID-19 classification based on CT images. *Bulletin of Electrical Engineering and Informatics*, *11*(5), 2876-2885.

[37] Ozturk, T., Talo, M., Yildirim, E.A., Baloglu, U.B., Yildirim, O., & Acharya, U.R. (2020). Automated detection of COVID-19 cases using deep neural networks with X-ray images. *Computers in biology and medicine*, *121*, 103792. https://doi.org/10.1016/j.compbiomed.2020.103792

[38] Ozyilmaz, A.T., & Bayram, E.I. (2023). Glucose-Sensitive Biosensor Design by Zinc Ferrite ($ZnFe_2O4$) Nanoparticle-Modified Poly (o-toluidine) Film. *Natural and Engineering Sciences*, *8*(3), 202-213.

[39] Panwar, H., Gupta, P.K., Siddiqui, M.K., Morales-Menendez, R., & Singh, V. (2020). Application of deep learning for fast detection of COVID-19 in X-Rays using nCOVnet. *Chaos, Solitons & Fractals*, *138*, 109944. https://doi.org/10.1016/j.chaos.2020.109944

[40] Patel, P. X-ray-dataset-2 (2020). *URL https://www.kaggle.com/prashant268/chest-xray-covid19-pneumonia*.

[41] Polsinelli, M., Cinque, L., & Placidi, G. (2020). A light CNN for detecting COVID-19 from CT scans of the chest. *Pattern recognition letters*, *140*, 95-100.

[42] Rahman, S., Sarker, S., Miraj, M.A.A., Nihal, R.A., Nadimul Haque, A.K.M., & Noman, A.A. (2021). Deep learning–driven automated detection of Covid-19 from radiography images: A comparative analysis. *Cognitive Computation*, 1-30.

[43] Rahman, T., Chowdhury, M., & Khandakar, A. (2020). Covid-19 radiography database. Kaggle, 2020.

[44] Rahman, T., Khandakar, A., Qiblawey, Y., Tahir, A., Kiranyaz, S., Kashem, S.B.A., & Chowdhury, M.E. (2021). Exploring the effect of image enhancement techniques on COVID-19 detection using chest X-ray images. *Computers in biology and medicine*, *132*, 104319. https://doi.org/10.1016/j.compbiomed.2021.104319

[45] Ronneberger, O., Fischer, P., & Brox, T. (2015). U-net: Convolutional networks for biomedical image segmentation. In *Medical Image Computing and Computer-Assisted Intervention–MICCAI 2015: 18th International Conference, Munich, Germany, October 5-9, 2015, Proceedings, Part III 18*. Springer International Publishing, 234-241.

[46] Sammut, C., & Webb, G.I. (2017). *Encyclopedia of machine learning and data mining*. Springer Publishing Company, Incorporated.

[47] Sarker, L., Islam, M.M., Hannan, T., & Ahmed, Z. (2020). COVID-DenseNet: A deep learning architecture to detect COVID-19 from chest radiology images. https://doi.org/10.20944/preprints202005.0151.v1

[48] Shan, F., Gao, Y., Wang, J., Shi, W., Shi, N., Han, M., & Shi, Y. (2020). Lung infection quantification of COVID-19 in CT images with deep learning. https://doi.org/10.48550/arXiv.2003.04655

[49] Sharma, A., Singh, K., & Koundal, D. (2022). A novel fusion based convolutional neural network approach for classification of COVID-19 from chest X-ray images. *Biomedical Signal Processing and Control*, *77*, 103778. https://doi.org/10.1016/j.bspc.2022.103778

[50] Sharma, P., Arya, R., Verma, R., & Verma, B. (2023). Conv-CapsNet: capsule based network for COVID-19 detection through X-Ray scans. *Multimedia Tools and Applications*, *82*(18), 28521-28545.

[51] Shichkina, Y.A., Kataeva, G.V., Irishina, Y.A., & Stanevich, E.S. (2020). The use of mobile phones to monitor the status of patients with Parkinson's disease. *Journal of Wireless Mobile Networks, Ubiquitous Computing, and Dependable Applications (JOWUA)*, *11*(2), 55-73.

[52] Singh, D., Kumar, V., Vaishali, & Kaur, M. (2020). Classification of COVID-19 patients from chest CT images using multi-objective differential evolution–based convolutional neural networks. *European Journal of Clinical Microbiology & Infectious Diseases*, *39*, 1379-1389.

[53] Soares, E., & Angelov, P. (2020). A large dataset of real patients CT scans for COVID-19 identification. *Harv. Dataverse*, *1*, 1-8.

[54] Soares, E., Angelov, P., Biaso, S., Froes, M.H., & Abe, D.K. (2020). SARS-CoV-2 CT-scan dataset: A large dataset of real patients CT scans for SARS-CoV-2 identification. *MedRxiv*, 2020-04.

[55] Song, Y., Zheng, S., Li, L., Zhang, X., Zhang, X., Huang, Z., & Yang, Y. (2021). Deep learning enables accurate diagnosis of novel coronavirus (COVID-19) with CT images. *IEEE/ACM transactions on computational biology and bioinformatics*, *18*(6), 2775-2780.

[56] Tingting, Y., Junqian, W., Lintai, W., & Yong, X. (2019). Three-stage network for age estimation. *CAAI Transactions on Intelligence Technology*, *4*(2), 122-126.

[57] Velichko, A. (2021). A method for medical data analysis using the LogNNet for clinical decision support systems and edge computing in healthcare. *Sensors*, *21*(18), 6209. https://doi.org/10.3390/s21186209

[58] Wang, L., Lin, Z.Q., & Wong, A. (2020). Covid-net: A tailored deep convolutional neural network design for detection of covid-19 cases from chest x-ray images. *Scientific reports*, 10(1), 19549. https://doi.org/10.1038/s41598-020-76550-z

[59] Wang, S., Kang, B., Ma, J., Zeng, X., Xiao, M., Guo, J., & Xu, B. (2021). A deep learning algorithm using CT images to screen for Corona Virus Disease (COVID-19). *European radiology*, *31*, 6096-6104.
[60] Wang, S., Zha, Y., Li, W., Wu, Q., Li, X., Niu, M., & Tian, J. (2020). A fully automatic deep learning system for COVID-19 diagnostic and prognostic analysis. *European Respiratory Journal*, *56*(2). https://doi.org/10.1183/13993003.00775-2020
[61] Wu, T., Tang, C., Xu, M., Hong, N., & Lei, Z. (2021). ULNet for the detection of coronavirus (COVID-19) from chest X-ray images. *Computers in Biology and Medicine*, *137*, 104834. https://doi.org/10.1016/j.compbiomed.2021.104834
[62] Xu, X., Jiang, X., Ma, C., Du, P., Li, X., Lv, S., & Li, L. (2020). A deep learning system to screen novel coronavirus disease 2019 pneumonia. *Engineering*, *6*(10), 1122-1129.
[63] Yasar, H., & Ceylan, M. (2021). Deep Learning–Based Approaches to Improve Classification Parameters for Diagnosing COVID-19 from CT Images. *Cognitive Computation*, 1-28.
[64] Zhang, J., Xie, Y., Pang, G., Liao, Z., Verjans, J., Li, W., & Xia, Y. (2020). Viral pneumonia screening on chest X-rays using confidence-aware anomaly detection. *IEEE transactions on medical imaging*, *40*(3), 879-890.
[65] Zheng, C., Deng, X., Fu, Q., Zhou, Q., Feng, J., & Decision, F. (2020). Deep Learning-based Detection for COVID-19 from Chest CT using Weak Label (preprint). https://doi.org/10.1101/2020.03.12.20027185

Authors Biography

Ahmad AL Smadi is an Assistant Professor at the Department of Data Science and Artificial Intelligence at Zarqa University. He completed his PhD degree in Computer Science and Technology from the School of Artificial Intelligence, Xidian University, Xi'an, China. He worked as a research assistant at the College of Technological Innovation, Zayed University, UAE. His research interests include information systems, computer vision, machine learning, and deep learning.

Dr. Ahed Abugabah is a Professor in Information Systems. He currently works at the College of Technological Innovation at Zayed University. Before joining Zayed University he worked in higher education in Australia where he received his degrees in information systems. His research interests include Information Systems, Enterprise Applications and Development, Machine Learning & Data Mining in Healthcare, Information Systems and RFID in Healthcare.

Mutasem K. Al-smadi is an associate professor affiliated with the College of Applied Studies and Community Service. He has made significant contributions of the field of research, particularly in the areas of Image Segmentation and Learning Management. With an h-index of 36, Dr. Alsmadi has achieved substantial recognition for his scholarly work. Throughout his academic career, Dr. Alsmadi has co-authored 81 publications that have garnered a remarkable total of 4,101 citations. His research output demonstrates both breadth and depth in addressing key challenges and advancing knowledge within the fields of Image Segmentation and Learning Management.

Ahmad Mohammad Al-smadi is a lecturer at Al-Balqa' Applied University (BAU), Jordan. He earned a Doctoral degree in Management Information Systems from Jinan University with distinction in 2016. His research interests encompass Information System Management, Business Intelligence, Decision Support Systems, and Artificial Intelligence. Dr. Al-Smadi has authored more than 10 scientific publications in peer-reviewed journals and conferences. Additionally, he has accumulated over 20 years of teaching experience at Al-Balqa' Applied University - Ajloun College.